# *Processes in Salt Repositories*

## Spent Fuel and Waste Disposition

***Prepared for***
***US Department of Energy***
***Spent Fuel and Waste Science and Technology***

**Kristopher L. Kuhlman**
*Sandia National Laboratories*

***June 7, 2019***
***M4SF-19SN010303035***

**DISCLAIMER**

This information was prepared as an account of work sponsored by an agency of the U.S. Government. Neither the U.S. Government nor any agency thereof, nor any of their employees, makes any warranty, expressed or implied, or assumes any legal liability or responsibility for the accuracy, completeness, or usefulness, of any information, apparatus, product, or process disclosed, or represents that its use would not infringe privately owned rights. References herein to any specific commercial product, process, or service by trade name, trade mark, manufacturer, or otherwise, does not necessarily constitute or imply its endorsement, recommendation, or favoring by the U.S. Government or any agency thereof. The views and opinions of authors expressed herein do not necessarily state or reflect those of the U.S. Government or any agency thereof.



Sandia National Laboratories is a multimission laboratory managed and operated by National Technology and Engineering Solutions of Sandia LLC, a wholly owned subsidiary of Honeywell International Inc. for the U.S. Department of Energy's National Nuclear Security Administration under contract DE-NA0003525.

Sandia
National
Laboratories

# Acknowledgments

The author acknowledges the group of salt researchers working on the topic at multiple locations (Sandia, Los Alamos, and Lawrence Berkeley national laboratories and at the WIPP site in Carlsbad). Discussions and topics from the DOE-NE Spent Fuel and Waste Science and Technology (SFWST) meeting in Las Vegas (May 21–23, 2019) and the Tenth US-German Workshop in Rapid City (May 28–29, 2019) are reflected in this report. The author thanks Tom Lowry and Emily Stein for reviewing the report.

This report satisfies a Level-4 milestone (`M4SF-19SN010303035`) in the DOE-NE SFWST Campaign in work package *"DR R&D – SNL"* and is report SAND2019-6441R.

# Contents

# List of Figures

# List of Tables

# Acronyms

| | |
|---|---|
| **CODE_BRIGHT** | COupled DEformation, BRIne, Gas and Heat Transport (Universitat Politècnic de Catalunya $\mathrm{TH^2MC_{PPT/DIS}}$ simulator) |
| **DOE** | US Department of Energy |
| **DOE-EM** | DOE Office of Environmental Management |
| **DOE-NE** | DOE Office of Nuclear Energy |
| **DRZ** | Disturbed Rock Zone |
| **EDZ/EdZ** | Excavation Damaged/disturbed Zone |
| **FEHM** | Finite Element Heat and Mass transfer (LANL $\mathrm{TH^2C_{PPT/DIS}}$ simulator) |
| **FEPs** | features, events, and processes |
| **FLAC** | Fast Lagrangian Analysis of Continua in 3D (Itasca Consulting Group $\mathrm{TH^1M}$) |
| **GDSA** | Geologic Disposal Safety Assessment |
| **LANL** | Los Alamos National Laboratory |
| **LBNL** | Lawrence Berkeley National Laboratory |
| **PA** | performance assessment |
| **PFLOTRAN** | Parallel reactive FLOw and TRANport ($\mathrm{TH^2C_{REACT}}$ simulator) |
| **SNL** | Sandia National Laboratories |
| **THC** | Thermal-Hydrologic-Chemical processes |
| **THM** | Thermal-Hydrologic-Mechanical processes |
| **THMC** | Thermal-Hydrologic-Mechanical-Chemical processes |
| **TM** | Thermal-Mechanical processes |
| **TOUGH2** | Transport Of Unsaturated Groundwater and Heat, version 2 (LBNL $\mathrm{TH^2C_{PPT/DIS}}$) |
| **US** | United States |
| **WIPP** | Waste Isolation Pilot Plant (DOE-EM site) |

# 1 Introduction

This report presents a discussion of processes relevant in a repository for heat-generating waste in geologic salt, from the point of view of coupled process models. This report is in essentially an update of Kuhlman (2014), in light of recent R&D in the DOE Office of Nuclear Energy (DOE-NE) Salt Disposal Research and Development program, including the heater test (Mills et al., 2019) being planned at the Waste Isolation Pilot Plant (WIPP).

Salt is widely considered a potential geologic medium for radioactive waste disposal, since in 1955 the US Atomic Energy Commission convened an expert panel to recommend best practices for radioactive waste disposal from the growing US nuclear weapons and power industries (Hess et al., 1957). Several candidate deposits of bedded and domal salt exist in the US (Johnson and Gonzales, 1978; Perry et al., 2014). US heat-generating radioactive waste is mostly solid used or spent fuel and high-level waste comprised of liquid reprocessing waste that either is or eventually will be turned into vitrified glass logs (Sandia National Laboratories, 2014). Permanent geologic disposal of solid radioactive wastes may involve placing waste casks or canisters into boreholes or into rooms mined in stable geologic salt deposits, with or without backfill. The Waste Isolation Pilot Plant (WIPP) is an operating, licensed geologic repository for transuranic defense waste in bedded salt in southeastern New Mexico, operated by the US Department of Energy (DOE) Office of Environmental Management (DOE-EM). This report discusses a hypothetical future repository for high-level radioactive waste relevant to the DOE Office of Nuclear Energy (DOE-NE), but data and knowledge gained from WIPP is invaluable in this goal.

Salt is considered a viable candidate medium for waste disposal because:

- Salt has high thermal conductivity ($\approx 5\ \mathrm{W/mK}$);
- Undisturbed salt has very low porosity ($\leq 0.1\%$), permeability ($\leq 10^{-22}\ \mathrm{m}^2$), and effective diffusion coefficient;
- Salt has no regional groundwater (evidenced by its geological stability);
- Hyper-saline brines are biologically simple (Nuclear Energy Agency, 2018) and have reduced colloid mobility;
- High chloride concentrations in brines reduce risk of criticality in breached packages;
- Salt can be mined easily and less expensively with a continuous miner and mined salt makes suitable backfill; and
- Fractures, damage, and backfilled salt will eventually close and heal to the same favorable properties as undisturbed salt.

Natural analogues provide one line of independent evidence to support claims regarding the long-term geological stability and viability of salt (Nuclear Energy Agency, 2014).

It is of central importance to understand and predict the availability of brine in salt surrounding radioactive waste (e.g., Kuhlman and Malama, 2013; Kuhlman and Sevougian, 2013; Kuhlman, 2014; Kuhlman et al., 2018). The availability of brine to excavations in salt is a function of the initial distribution of water in salt, and the distribution of damage around the excavation provides the porosity and permeability that allows brine to move.

## 1.1 Brine in Salt

Figure 1.1 illustrates the relationship between the three primary water forms in bedded rock salt, intergranular and intragranular brine. We consider three brine types (listed in order of significance):

- Water of hydration chemically bound to hydrous minerals, including polyhalite, gypsum, and intercalated water in clays (Roedder and Bassett, 1981; Caporuscio et al., 2013);
- Intragranular brine (i.e,. fluid inclusions); and
- Intergranular (i.e., grain-boundary or pore) fluids, including brine saturating the porosity in clay and anhydrite layers.

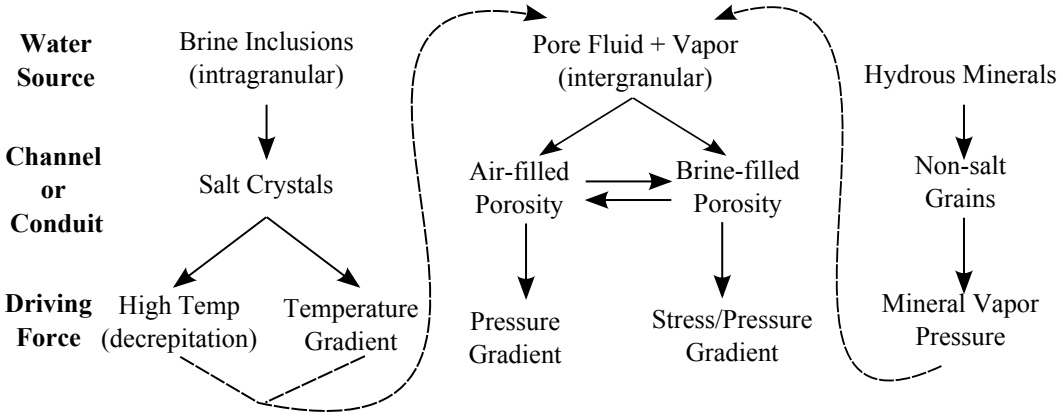


**Figure 1.1. Types of brine and migration mechanisms (Shefelbine, 1982; Kuhlman, 2014)**

Water in hydrous minerals is the largest reservoir of water in most bedded salt deposits (including intercalated water in clay minerals), but this water is not available to flow under pressure gradients and is only released when the minerals are heated to their dehydration temperature. Fluid inclusions are the next most abundant form of water in bedded salt, which are also not available to flow under a pressure gradient, they are released to intergranular porosity through heating or damage. Although intergranular brine is the smallest portion of water in geologic salt, the pore network it occupies is the main pathway from the far field to the excavation (Figure 1.1). The significance of brine flow due to pressure gradients through connected intergranular porosity has been shown in numerous field and laboratory studies.

Early laboratory permeability testing in the 1950s and 1960s illustrated linear Darcy-type porous media flow under a pressure gradient through salt cores from the Grand Saline salt dome mine (Reynolds and Gloyna, 1960; Gloyna and Reynolds, 1961). Recent studies of low-permeability rocks have often shown a threshold gradient, which can lead to non-Darcy flow (Liu and Birkholzer, 2012). From the 1960s to the mid-1980s, much of the research on brine movement in salt focused on migration of intragranular fluid inclusions under temperature gradients.

A historic surge in fluid inclusion research was fueled by field and laboratory observations made during Project Salt Vault (Bradshaw and Sanchez, 1969; Bradshaw and McClain, 1971). Data collected during project Salt Vault was fitted by Jenks (1979) using a simple exponential model, which saw wide application. Rübel et al. (2013) surmised the Jenks (1979) model was fitted to anomalous data, making most subsequent applications of this model inappropriate.

A thermoporoelastic conceptual model for intergranular brine flow in salt has been successfully applied to unheated and heated brine transport at WIPP (McTigue, 1986, 1990; Beauheim et al., 1997). Hadley (1982) developed an alternative conceptual model for vapor flow from an evaporation front. These models assumed liquid or vapor movement in connected intergranular porosity and left out intragranular fluid inclusions to simplify mathematical and numerical models. Olander et al. (1982) developed a conceptual model including both intergranular vapor flow and intragranular fluid inclusion movement. Ratigan (1984) developed a numerical model including intragranular fluid inclusions and intergranular brine flow, but it did not include thermal expansion effects on the intergranular porosity. Current numerical models for brine flow in granular salt assume a porous continuum (e.g., FEHM, TOUGH2, PFLOTRAN) with water moving under liquid and vapor pressure gradients. Most numerical models do not incorporate fluid inclusions along with intergranular brine and vapor migration. Rutqvist et al. (2018) has illustrated an implementation of fluid inclusion migration with intergranular brine and vapor flow via a dual-porosity conceptual model using TOUGH2.

## 1.2 Coupled THMC Processes in Salt

The general nature of Thermal, Hydrological, Mechanical, and Chemical (THMC) salt behavior has been known since the late 1950s (Hess et al., 1957; Serata and Gloyna, 1959; Reynolds and Gloyna, 1960), but the details regarding the coupled processes and constitutive laws have only been understood and confirmed since large-scale heated brine migration field and laboratory tests in the 1980s at Asse, WIPP, and Avery Island (Sherer, 1987). Numerical modeling of coupled processes (Figure 1.2) an active area of research in repository science (Tsang, 2009), reservoir geomechanics (Zoback, 2007; Prevost, 2014), carbon sequestration, among other earth science fields (Herrera and Pinder, 2012), leading to the development of generic modeling tools for numerical simulation of coupled processes.

At proposed mined repository depths ($\leq$ 1 km depth) and thermal loads ($<$ 10W to a few kW per canister; Sandia National Laboratories, 2014) thermal, hydrological, mechanical, and chemical (THMC) processes become all relatively important and coupled with one another. Except under special experimental designs or restrictive circumstances, we cannot predict in isolation a single process from a THMC experiment without significant error and loss of physical significance. The thermal-mechanical (TM) problem in salt is characterized by the strong dependence of mechanical properties on temperature; higher temperature reduces salt's effective viscosity. The

| Type | Example |
|---|---|
| T = C | phase changes |
| T = H | buoyancy flow |
| T = M | thermally induced fractures |
| H = C | solution and precipitation |
| H = M | hydraulic fracturing |
| C–M | stress corrosion |
|  | chemical reactions and transport in hydrothermal systems |
|  | thermomechanical effects with change of mechanical strengths due to thermochemical transformation |
|  | thermally induced hydromechanical behavior of fractured rocks |
|  | hydromechanical effects (in fractures) that may influence chemical transport |
|  | chemical reactions and transport in fractures under thermal and hydraulic loading |

**Figure 1.2. Examples of THMC couplings for a generic repository. Lines are couplings, double lines are strong couplings (Tsang, 1987)**

thermal-hydrological-mechanical (THM) problem in salt (Figure 1.3) is characterized by strong dependence of salt's hydraulic properties on mechanical deformation, migration of fluid inclusions, effect of pore pressure on stress, along with the differential thermal expansion of salt and brine. Chemical effects further complicate the THM representation, with additional coupling due to the precipitation and dissolution of salt in the pore space and creation of heat pipes around heat sources in granular salt.

We do not consider biological effects, since they would likely be slight for a salt repository, where the activity of water is $< 0.75$, which makes it difficult to maintain all but halophilic life (Nuclear Energy Agency, 2018). We also do not consider radiological processes inside the waste form, which may be more important for large waste packages, like direct disposal of dual purpose (i.e., storage and transportation) canisters (Hardin et al., 2013, 2015).

## 1.3 Process vs. PA Models

In the context of a repository safety case, a process model is any model that simulates one or more processes occurring in the engineered or natural components of a repository system. In salt repositories processes include: brine, gas, and heat flow; advective and dispersive transport of solutes including radionuclides; chemical reaction such as waste package corrosion and mineral

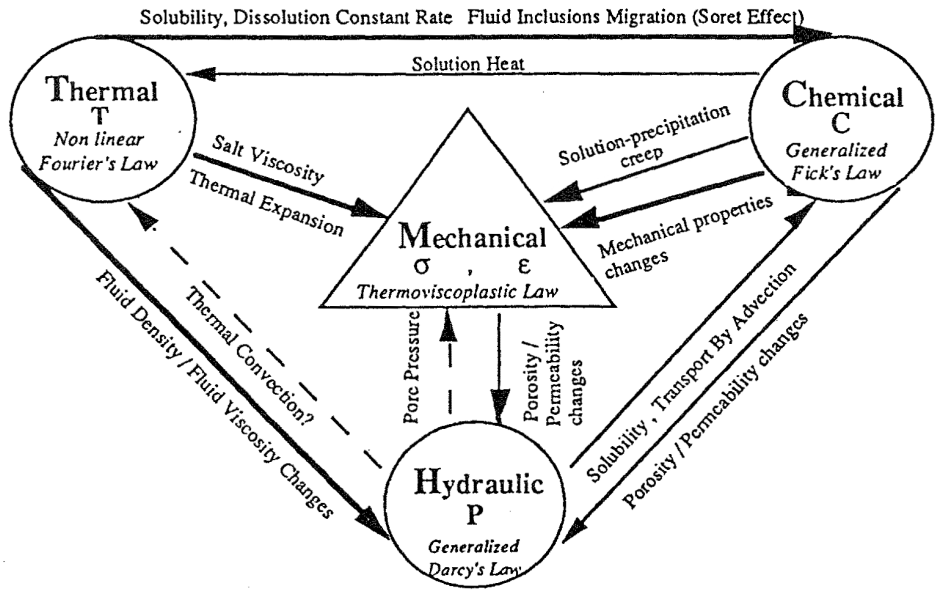


**Figure 1.3. Illustration of THMC couplings in salt (Cosenza and Ghoreychi, 1993)**

precipitation and dissolution; and visco-plastic and elastic deformation of the salt surrounding the excavation. Process models may be developed for stand-alone simulations aimed at improving understanding of the processes occurring in the repository system or developed for incorporation in performance assessment (PA) models, the goal of which is to predict the probability of release of radionuclides from the repository to the biosphere or to the accessible environment.

Process models are used to simulate a wide range of time and space scales, but are often validated against data collected where things are changing fastest (early time after waste emplacement) and have the steepest gradients (in and immediately around the mined drift). Challenges of scale arise when integrating process models into PA simulations due the coupling between far field transport processes occurring over long time (thousands to millions of years) and distance (kilometers) scales and near field processes occurring over short time (up to hundreds of years) and distance (up to meters) scales. Because PA simulations include Monte Carlo style uncertainty analysis, the need for computational efficiency poses an additional challenge, which may be addressed by using coarser solution meshes or simplified physics in comparison to a stand-alone process model.

Despite these challenges, integration of near-field process models is important to performance assessment of a salt repository because near-field processes affect:

1. pressures, saturations, concentrations, and fluxes through high-permeability or porous pathways (i.e., natural or human-made pathways, both pre-existing or only in hypothetical future scenario);

2. the evolution of properties that affect radionuclide transport, including porosity, tortuosity, permeability, and pore-size distribution of crushed salt backfill, shaft seals, and EDZ;

3. the evolution of properties that affect radionuclide release, including near-package chemical composition, waste package corrosion rates, waste form dissolution rates, radionuclide sorption, and radionuclide solubility.

Process models that have significant impact on radionuclide release and transport must be integrated into PA models in a manner robust enough for meaningful prediction and computationally efficient enough for probabilistic uncertainty quantification. Such integration will rely on some combination of fully mechanistic modeling, reduced order and surrogate modeling, and multiscale coupling. Stand-alone process models that predict in-drift evolution of the system during pre-closure and early post-closure times may also be used to predict initial conditions for PA models. or may be used to "screen out" some physical processes from PA models as unimportant with respect to radionuclide release and transport.

The Geologic Disposal Safety Assessment (GDSA) Framework relies on PFLOTRAN, a massively parallel multiphase flow and reactive transport simulator, for simulation of the coupled thermal-hydrological-chemical (THC) processes occurring in a repository system (Freeze et al., 2013). To date, GDSA PA reference case simulations of generic repositories in bedded salt have neglected some of the processes that may influence radionuclide release and transport. For instance, the GDSA simulations assume step changes in the porosity and permeability of the crushed salt backfill, rather than simulating the fully coupled, thermal-hydrological-mechanical-chemical (THMC) processes necessary to compute these hydrologic variables in response to an evolving system state (Mariner et al., 2015; Sevougian et al., 2016).

Compared with other possible disposal media (e.g., crystalline or argillite), numerical models of salt repositories must account for:

- increased containment and reduction of release in undisturbed scenarios due to the very low porosity and permeability in the far field (GDSA/PA models) and
- added complexity in the near field due to THMC coupling, mineral solubility, and complex creep behavior (process models).

The next chapter discusses processes that are or could be included in process and PA models. Typically a process would first be included in a process model to test its impacts on model predictions, then later could be included in PA models. The decision to include processes in PA models that increase model run time or complexity must be made carefully. The decision to simplify or leave a process out of PA models should also be made carefully, and is often times documented through the Features, Events and Processes (FEPs) procedure. Processes featured in ongoing research may one day be included in future PA models, beyond those included in the WIPP PA model (DOE, 2014), in previous GDSA models (Mariner et al., 2015; Sevougian et al., 2016), or in the German safety case for Gorleben (Bollingerfehr et al., 2013).

# 2 Salt Repository THMC Processes Conceptual Model

Our conceptual model includes the excavated drift, and the waste packages emplaced there, as well as the undisturbed far field. The extent and nature of the transition between the near- and far field is more difficult to define a priori. For this report, we distinguish between the excavation *damaged* zone (EDZ), where material properties have been altered, and the excavation *disturbed* zone (EdZ), where only the state variables have changed (Figure 2.1). Because mechanical damage to salt will eventually heal, these zones will shrink with time; their maximum extent is their typical definition.

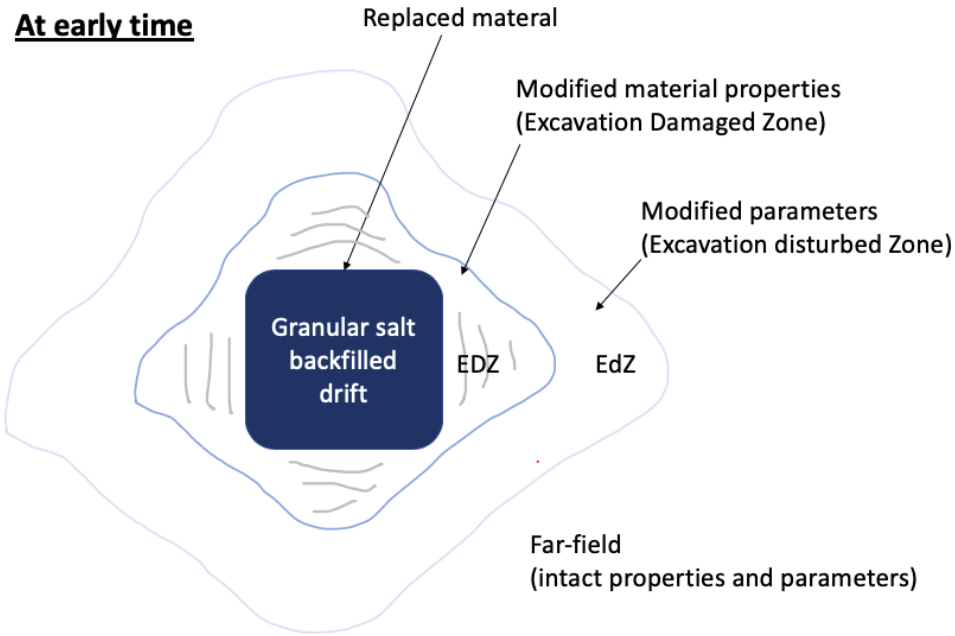


**Figure 2.1. Definitions of EdZ and EDZ regions in salt repository conceptual model**

For this report, we consider multiple EDZ and EdZ to exist, as many as one for each process. A thermal EDZ would be where the thermal transport properties have been modified, and the thermal EdZ would be where the temperature has been perturbed from background. Obviously with coupling between the processes, these definitions can become somewhat circular or arbitrary.

The processes are presented in a generic enough way to cover processes in the near field and in the far field, but most processes are not relevant everywhere. We present the key properties and variables to be considered at a high level.

| Process | EDZ-defining Properties | EdZ-defining Variables |
|---|---|---|
| Thermal | thermal conductivity, heat capacity, fluid flow velocity, porosity | temperature |
| Hydrological | permeability, porosity, non-Darcy parameters | fluid pressure, saturation, fluid density, fluid flow velocity |
| Mechanical | moduli, creep constitutive law parameters, interface slip parameters | stress, strain (porosity), damage |
| Chemical | tortuosity, porosity, flow velocity | water activity, species concentrations (solid, liquid and sorbed phases) |

**Table 2.1. Process-specific EDZ and EdZ**

Since we cannot represent the entire subsurface in our simulations, we must truncate the domain at some convenient distance from the repository. The size of the domain required increases with the length of the simulation. PA simulations require larger domains than process model simulations. Setting up initial conditions, especially in simulations with coupled processes, must be considered carefully. Often one simulation must be performed to derive a consistent (i.e., steady-state) set of inputs for a repository model.

## 2.1 Thermal Processes

The primary thermal variable is temperature ($T$), which is increased above the background temperature (i.e., geothermal gradient) by the energy output from radioactive waste decay. It is highest near the waste package immediately after emplacement, and is lowest in the far field away from the effects of the repository.

### 2.1.1 Heat Conduction

Heat conduction due to a temperature gradient is the dominant energy transport mechanism in the far field, where porosity and permeability are low. It is the only energy transport mechanism through non-porous salt crystals (i.e., it does not require connected pore space):

$$\frac{1}{\alpha_T}\frac{\partial T}{\partial t} = \nabla^2 T.$$

Thermal diffusivity ($\alpha_T = k_T/(\rho c_v)$) is the ratio of thermal conductivity ($k_T$) and heat capacity ($C_v$) times density ($\rho$). It is not significantly different in the EDZ and in the far field (Cosenza, 1996); both $k_T$ and $\rho C_v$ are lower in the backfilled drift than in intact rock. In granular salt, thermal conduction becomes less effective because the run-of-mine salt is up to 40% porosity (significant thermal gradients in fluid-filled spaces will usually initiate convection).

For numerical models, the initial conditions (before heat-generating waste emplacement) is a geothermal gradient increasing temperature with depth. Boundary conditions could be specified-temperature near the top of the domain, and either a specified-temperature or specified heat flux

at the bottom of the domain. Before the waste is emplaced, there is heat conduction occurring; energy is being conducted up from warmer rocks at depth to the cooler surface.

We represent the thermal boundary condition at these edges of the domain as either specified temperature (type I) or specified flux (type II). If we represent them as specified temperature, we will *underestimate* impacts of the repository in the far field (since temperature is fixed there). If we represent them as specified flux or insulated, we will *overestimate* impacts of the repository in the far field (since flux is fixed there). The most physically realistic option is to make the model domain larger, until a physical boundary is reached or the impacts of the repository do not reach the model boundaries, but this could lead to very large model domains.

### 2.1.2 Heat Convection

Convection occurs when energy is moved by either gas- or liquid-phase transport through pore spaces. Convection, when viable, can be a far more efficient mechanism for energy transport than conduction, but it can only occur through a connected pore space, and requires a moving fluid (gas or liquid). Heat pipes are a type of free convection cell (Figure 2.2) that is possible in the near field, when high temperatures cause boiling of brine and drive vapor transport of enthalpy (i.e., internal energy + pressure × volume) away from the heat source:

$$\rho C_v \frac{\partial T}{\partial t} = k_T \nabla^2 T + \vec{u} \nabla T$$

where $\vec{u}$ is the Darcy flow vector.

The pore flow velocity of brine or vapor driving convection ($\vec{u}$) varies significantly between the drift, EDZ, and the far field (see Hydrological Processes subsection). In the far field there is very little connected porosity and no convection of energy (i.e., if there is any convection through the tiny pore space, it is minor compared to heat conduction through the solid salt). Convection in the drift, through granular salt, can be quite significant, due to the high porosity and permeability of granular salt, and the proximity to the heat source which can drive free convection. A heat-pipe can form, where hot vapor caries energy away from the heat source efficiently (lower temperature gradients than heat conduction), precipitating salts and reducing the porosity where the brine boils away.

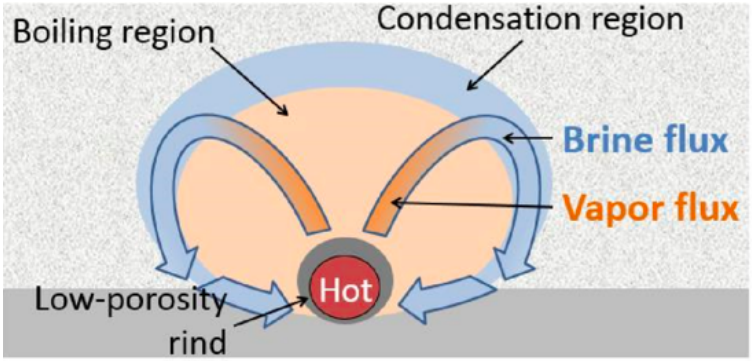


**Figure 2.2. Illustration of heat pipe around a hot waste package in granular salt**

When the vapor gets to a cooler region, it can condense and dissolve salt (increasing the porosity where the condensation happens). If heat conduction is the only mechanism for thermal energy

transport in the near field, the temperature at the heat source will be hotter than in a system with free convection (Figure 2.3).

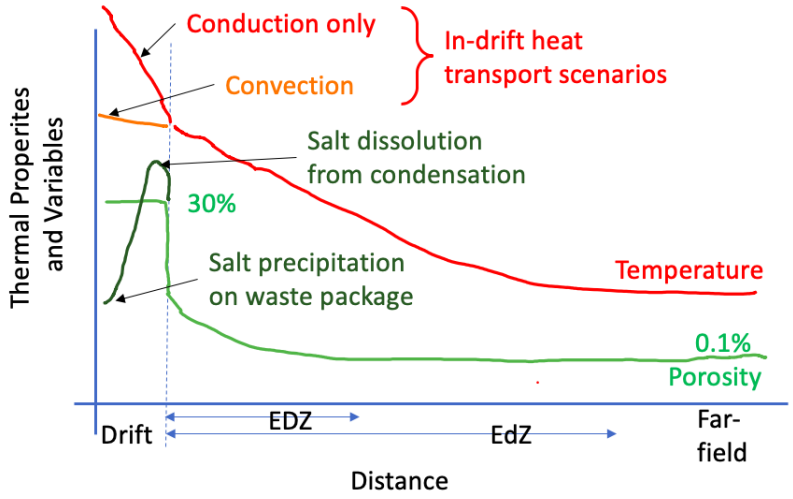


**Figure 2.3. Conceptual trends in temperature under conduction and convection scenarios**

The initial condition for convection is no regional liquid or gas flow, and therefore no thermal convection. Previous GDSA simulations have included minor lateral regional hydrologic flow (Mariner et al., 2015; Sevougian et al., 2016), but this does not convect energy because it is perpendicular to the spatially uniform geothermal gradient. Thermal convection is solely due to the perturbation of the repository. The boundary conditions applicable to the regional hydrological flow problem drive thermal convection. Even if there is some component of regional groundwater circulation to drive convection, there will be minimal regional steady-state energy convection. Convection is typically not a controlling factor on required domain size, since for very low flow velocities, thermal conduction is much more efficient. Any slight thermal convection will be negated by a counter-flow of conduction that evens out any convective temperature difference.

Kuhlman (2014) presented an analysis based on dimensionless parameters, which illustrated how the thermal Peclet number changes from the near to far field, illustrating how the problem goes from convection dominated in the near field to conduction dominated in the far field.

### 2.1.3 Radiation

Radiation only occurs in open spaces (i.e., high porosity). It can be a very efficient and important energy transport mechanism where large temperature differences exist in an open borehole or drift, but is not considered here because the GDSA reference case assumes all openings are back-filled with porous materials. Some models for heat transfer in granular salt include terms that approximately include the effects of radiation, but the impact of this is slight unless temperature gradients are very steep (Lerch, 2019).

## 2.2 Hydrological Processes

The primary hydrological variables are fluid pressure ($p$, liquid or gas phase pressures) and the relative amount of each phase ($S$ saturation occupying the pore space). Figure 2.4 illustrates the trends in hydrological properties and variables. In the far field the small amount of pore space is liquid saturated (no connected gas phase) and the liquid pressure is equal to the lithostatic pressure (e.g., at WIPP the repository is at 650 m depth and 15 MPa lithostatic pressure). In the drift, the system is nearly gas saturated (limited brine) and the gas pressure is essentially equal to atmospheric pressure (0.1 MPa). There is a very steep gradient in saturation and fluid pressure going away from the drift into the far field, which is supported by the low permeability and porosity of the salt. If the salt were more permeable, brine would flow and dissipate the steep pressure gradient, extending the EdZ much further away from the excavation. $H^1$ and $H^2$ indicate single- or two-phase hydrologic processes in acronyms like $TH^1C$ or $TH^2C$.

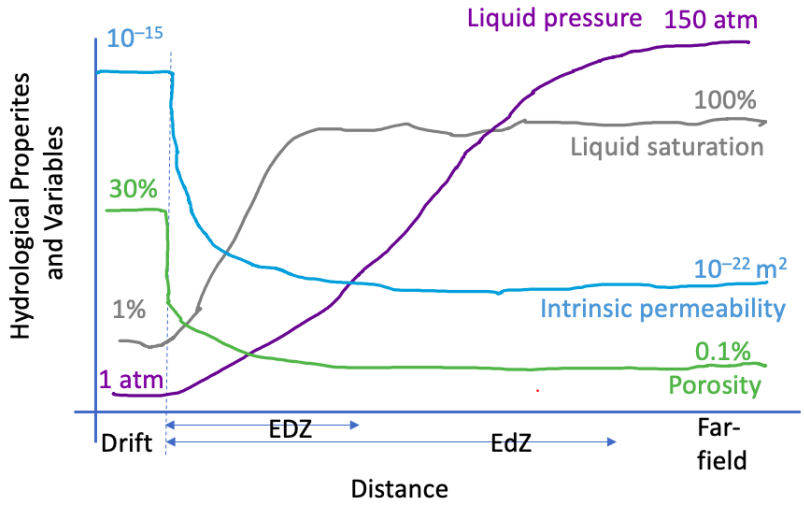


**Figure 2.4. Conceptual trends in hydrological properties and variables around an excavation**

The following subsections describe contributing driving factors in hydrologic flow: pressure-driven flow, capillarity-driven flow, gravity-driven flow, and the material properties that control hydrological flow.

### 2.2.1 Pressure-driven Flow

Darcy flow is fluid flux through a porous media, down a pressure gradient. Flux of gas or liquid can occur if a continuous phase exists in the pore space and a pressure gradient is maintained,

$$\vec{u}\phi = \vec{q} = \frac{kk_r}{\mu}\nabla\left(p + \rho g z\right)$$

where $\phi$ is porosity, $\vec{q}$ is Darcy flux (over the bulk of the whole rock), $\mu$ is liquid viscosity, $k_r$ is relative permeability, $k$ is the intrinsic permeability tensor, $g$ is gravitational acceleration, and $z$ is elevation.

The flow of brine or vapor varies significantly between the open drift and the far field. In the far field there is no gas flow (because there is no connected gas-filled porosity) and no liquid flow due to low intrinsic permeability. In the near field there can be significant short-range flow of both gas and liquid through the porosity.

In low-permeability rocks, non-Darcy flow has been observed (Liu and Birkholzer, 2012; Liu, 2014), where a threshold gradient ($I$ in Figure 2.5) must be overcome to achieve a typical Darcy flux. This non-Darcy flow mechanism would yield zero or lower regional groundwater flow than would be found by simply applying Darcy's law with the regional gradient and permeability. One proposed non-Darcy expression for flux in terms of pressure gradient is (Liu, 2014)

$$\vec{q} = \frac{kk_r}{\mu}\left[i - I\left(1 - e^{i/I}\right)\right],$$

where $i = \nabla\left(p + \rho g z\right)$ is the hydraulic gradient. Although there is no salt-specific field data to support this, it is conceptually consistent with geologic stability of salt deposits, which would dissolve if regional groundwater flow were significant. This assumption was made in Germany for the Gorleben radioactive waste disposal reference case (Bollingerfehr et al., 2013). In the German safety case, there is no far-field hydrological flow beyond the permeability associated with damage from excavating the repository.

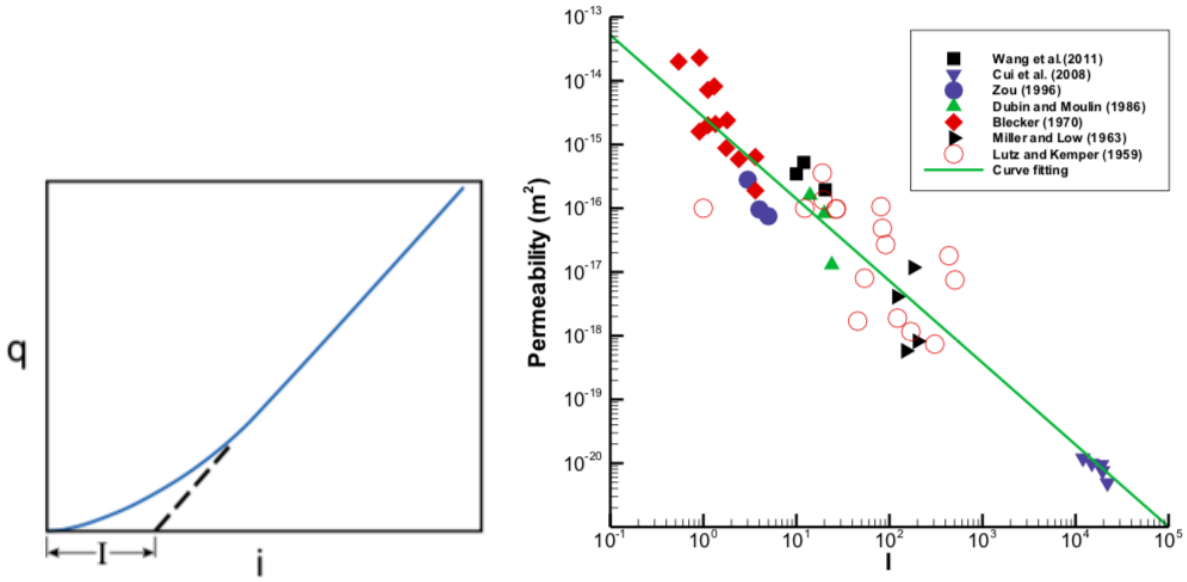


**Figure 2.5. Relationship (left) between Darcy flux ($q$), applied gradient ($i = \nabla(p + \rho g z)$), and threshold gradient ($I$), and data (right) showing estimated threshold gradient and relationship to intrinsic permeability (Liu, 2014)**

The regional boundary condition for Darcy flow is often simulated by an imposed fluid pressure difference between two vertical sides of the domain to create lateral flow. The evidence for a lack of regional groundwater circulation in salt indicates the non-disturbed permeability of salt is low enough (with or without non-Darcy flow mechanisms) in the far field to prevent steady-state circulation.

The initial condition for single-phase Darcy flow is the pressure distribution. The liquid pressure in the far field may be as high as lithostatic, since salt cannot support a deviatoric stress over geologic time. At equilibrium all the stresses in the salt are equal to lithostatic. The fluid pressure in the salt can be up to lithostatic pressure (if it were higher it would lead to hydrofracture and dissipation of pressure). Field data from WIPP (Beauheim and Roberts, 2002) indicate the far-field static formation pressure is approximately 12–15 MPa (hydrostatic to lithostatic pressure at a depth of 650 m).

The initial condition of brine formation pressure around an excavation can be simulated via the relief of pressure around the excavation from the initial state, either using a hydrologic model (e.g., Figure 2.6) or a coupled hydro-mechanical model (e.g., Rutqvist et al., 2018).

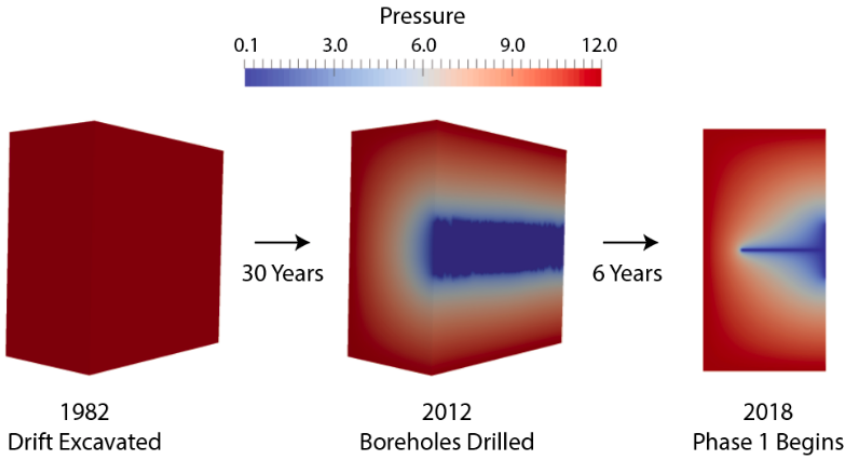


**Figure 2.6. Development of hydrological initial condition around boreholes in salt at WIPP from an undisturbed initial condition (Stauffer et al., 2019)**

As a TH coupled effect, thermal pressurization can happen at the edge of the hydrologic EDZ, if the temperature rise is high enough to cause significant volume expansion of the pore fluids, but the intrinsic permeability is low enough to prevent the liquid pressure from dissipating (Figure 2.7). In $TH^2$, liquid saturation must also be nearly 100% for thermal pressurization, or the more mobile residual gas will migrate due to the pressure of the liquid expansion.

If the temperature rise from the repository (i.e., the thermal EdZ) extends out further than the hydrologic EDZ (the region where permeability and porosity are increased) and the hydrologic EdZ (the region where fluid pressure is undisturbed and the liquid saturation is unity), the thermal pressurization of the fluid could locally bring liquid pressure above lithostatic pressure, leading to hydrofracture and dissipation of the excess pressure towards the excavation. Therefore the hydrologic EdZ is larger or approximately the same size as the thermal EdZ, since the hydrologic EDZ would grow in size due to hydraulic fracture if thermal pressurization exceeded lithostatic pressure.

### 2.2.2 Capillarity-driven Flow

Capillarity's effects on flow are not separate hydrological processes, they are contributing factors in two-phase Darcy flow ($H^2$), but for clarity it is discussed here individually. Capillary pressure

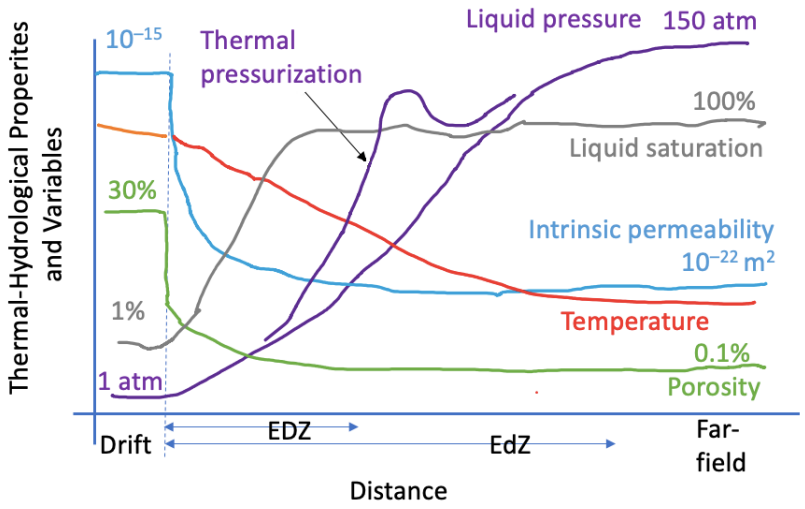


**Figure 2.7. Conceptual trends in TH processes, including thermal pressurization**

represents the pore-scale effect that surface tension in small pores has on the balance between gas and liquid pressures, and is given by

$$p_c = p_{\text{air}} - p_{\text{brine}}$$

where it is assumed brine is the wetting fluid, and air is the non-wetting fluid.

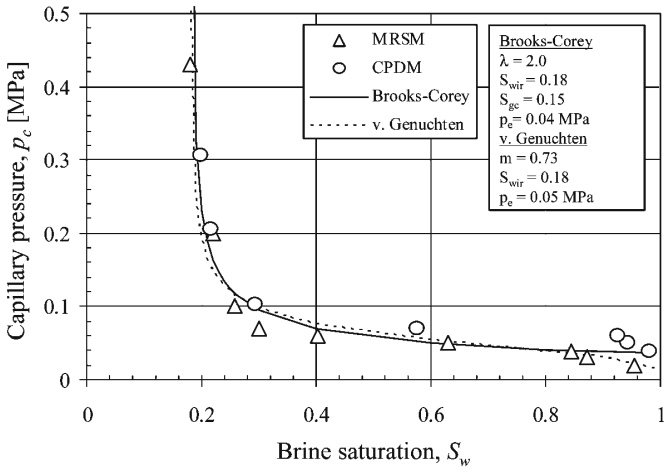


**Figure 2.8. Capillary pressure data and moisture retention curve for granular salt (Cinar et al., 2006)**

The capillary pressure relationship illustrated in Figure 2.8 for granular salt shows the competing flow of both brine and gas through the same pore space. This relationship can be used to predict $k_r$ as a function of saturation if no data exist. Capillarity can wick brine (i.e., the wetting fluid) into a porous or fractured medium, or prevent air (i.e., the non-wetting fluid) from entering brine-saturated fractures and pores below the air-entry pressure. When the porosity gets very high (i.e., in an open drift), capillarity is reduced (Johnson et al., 2019); the maximum capillary

pressure in an open space is much lower than that in small pores or fractures. Capillarity is also reduced when salinity increases – but in a salt repository brine is often considered to be equally hyper-saline (but see discussion in Section 2.4). Capillarity is also reduced at higher temperatures, due to the decrease in water surface tension with temperature.

In the far field, flow is essentially single-phase (brine only), so the initial condition there does not involve capillarity. Capillary effects are limited to the perturbation around the excavation (Kuhlman, 2014). The saturation distribution around an excavation is related to the damage distribution. The salt is low-permeability and brine-saturated in the far field, the mechanical damage which increases the absolute permeability and porosity near an excavation simultaneously decreases the liquid saturation near the excavation. The decrease in relative permeability in the DRZ may cancel out any increases in absolute permeability, creating a vapor barrier near the excavation, reducing the ability of brine to flow into an excavation.

There is little capillary pressure data available for salt. The little amount of data that exists is for uniform granular salt (i.e., table salt). Cinar et al. (2006) presented a study of the petrophysical properties of fine-grained crushed salt (Figure 2.8) and Olivella et al. (2011) included experimental capillary pressure data in their precipitation/dissolution laboratory modeling study. Important parameters related to two-phase flow behavior and capillary pressure are the gas-threshold and air-entry pressures ($P_{\mathrm{gt}} = P_{\mathrm{e}} + P_{\ell}$, where $P_{\mathrm{gt}}$ is gas-threshold pressure, $P_{\mathrm{e}}$ is the air-entry pressure, and $P_{\ell}$ is the liquid or formation pressure). Air-entry pressure is that required for air to enter a liquid-saturated sample (Davies, 1991). It can be estimated through laboratory or field experiments, but is often empirically related to permeability or pore/fracture aperture (Figure 2.9). Lower permeability materials tend to have high air-entry pressure, since both parameters are related to the pore radius or fracture aperture.

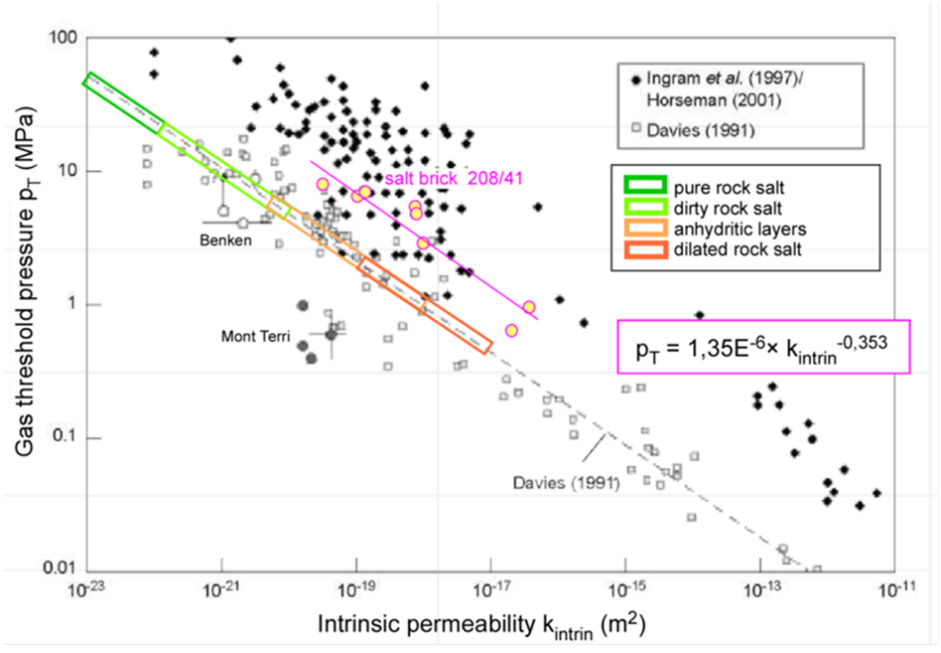


**Figure 2.9. Permeability and gas-threshold pressure (Salzer et al., 2007)**

The pore space in the EDZ is mostly gas-saturated (Figure 2.10), but this initial condition can be difficult to set up. Given the brine-saturated far-field, one option is to drain a brine-saturated

model domain until an equilibrium around the excavation is reached. The other option is to create porosity around the excavation at lower brine saturation, and let imbibe brine into an initially numerical model from the far field. The drainage approach to setting up hydrological models runs faster, but will result in unrealistically initial high brine saturation in the EDZ (Kuhlman, 2014).

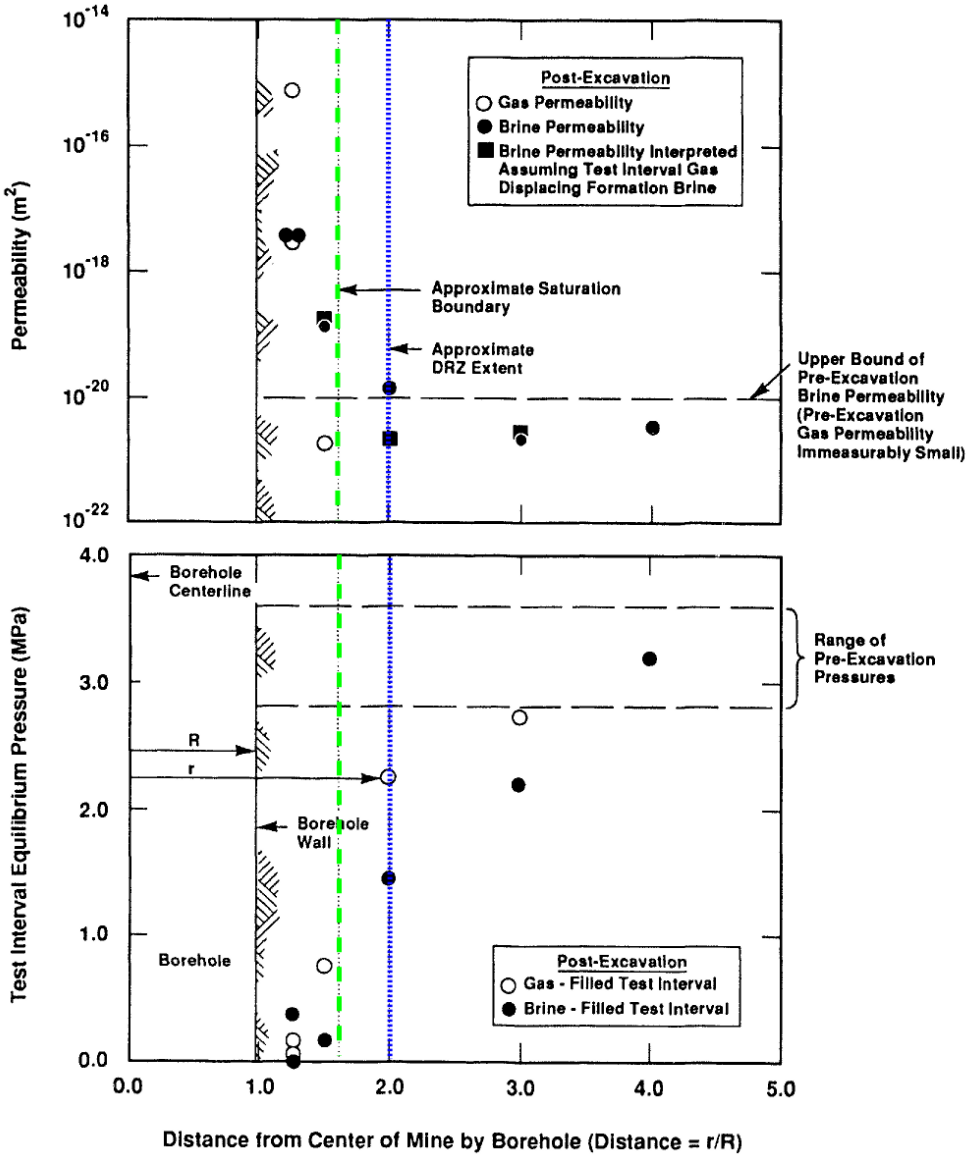


**Figure 2.10. WIPP small-scale mine-by experiment results showing extent of mechanical EDZ (blue dotted line) and hydrological EdZ (green dashed line) (Stormont et al., 1991)**

## 2.2.3 Gravity-driven Flow

Gravity's effects on flow also are not a separate processes, they are contributing factor to density-driven flow. Gravity effects become significant where two fluids of different densities exist in a pore space (i.e., gas and liquid, or brines of different ionic strengths), leading to free fluid convection

(which can drive energy convection). An increase in temperature reduces the density of liquids (gas densities are more impacted by pressure). Changes in density can also occur due to temperature-dependent changes in mineral solubility and resulting changes in ionic strength.

Multiphase flow simulations can track the drainage of liquid under gravity or the rising of gas through a liquid-saturated medium. Coupled $\mathrm{TH}^2$ models can track the effects of free convection due to thermal expansion and coupled $\mathrm{TH}^2\mathrm{C}$ models can track the impacts dissolution and precipitation of solutes has on the density of the liquid phase. Gravity can drive brine to accumulate in the EDZ below an excavation, or cause gas to rise up in the EDZ above an excavation.

In the far field, flow is essentially single-phase and brine is assumed to be of uniform density, so the initial condition does not typically involve gravity. Gravity effects are typically limited to the perturbation around the excavation, and are often ignored in the far field. Boundary conditions in numerical models may be impacted by gravity or density effects: imposing a geothermal temperature gradient or a salinity gradient along a boundary can lead to different-than-hydrostatic pressure distributions. Density effects may stabilize regional groundwater flow systems near the edge of salt deposits. The density and viscosity of dense brine may prevent the mixing of fresh meteoric groundwater from above (Freeze et al., 2019). The effect may be more important around the edges of salt domes or at the fringes of a bedded salt deposit.

### 2.2.4 Fluid Inclusion Migration

It is well known that single-phase fluid inclusions migrate towards a heat source (up a thermal gradient), while bi-phase fluid inclusions can migrate away from a heat source (down a thermal gradient). One explanation for this phenomenon is the temperature dependence of solubility of salt; the difference in temperature across a fluid inclusions ($\approx$ 2 mm) is enough to dissolve salt from one side of the inclusion and precipitate it on the other – moving the fluid inclusion. In bi-phase inclusions water vapor is more mobile than dissolved salt, so evaporation and condensation produce a salinity gradient that moves the inclusion. Steep thermal gradients must be maintained to keep fluid inclusions migrating; these steep thermal gradients only exist close to a heat source. In intact salt, fluid inclusions may become intergranular brine or move into adjacent crystals or stop migrating when they encounter a mineral other than halite. In granular salt, fluid inclusions would flow into the connected (typically air-filled) pore space. Increasing the temperature beyond the decrepitation point will liberate the intragranular brine through shattering of the salt crystal under the stress of expanding brine and high brine vapor pressure.

### 2.2.5 Hydrological Properties

Permeability, porosity, tortuosity, and pore-size distribution (i.e., two-phase flow properties) are hydrological properties that vary significantly from the EDZ to the far field.

Intrinsic permeability and porosity increase significantly around an excavation over their very low, undisturbed far-field values. The intrinsic permeability of the EDZ can be several orders of magnitude higher than the far field, and the porosity of the EDZ can be a factor of 10 or 20 higher than the far field (Figure 2.11). During drift closure and healing of the damage associated with the excavation, the porosity will be reduced – eventually back to the undisturbed state. Permeability will also be reduced during healing, but the relationship between porosity and permeability is not a simple linear relationship (even on log-log scale; Kuhlman and Matteo, 2018). Sometimes a

small change in porosity can lead in a huge change in permeability, depending on the connectivity of the porosity. Permeability in the EDZ surrounding a room is also directional, with fractures preferentially forming parallel to the drift walls (Figure 2.1).

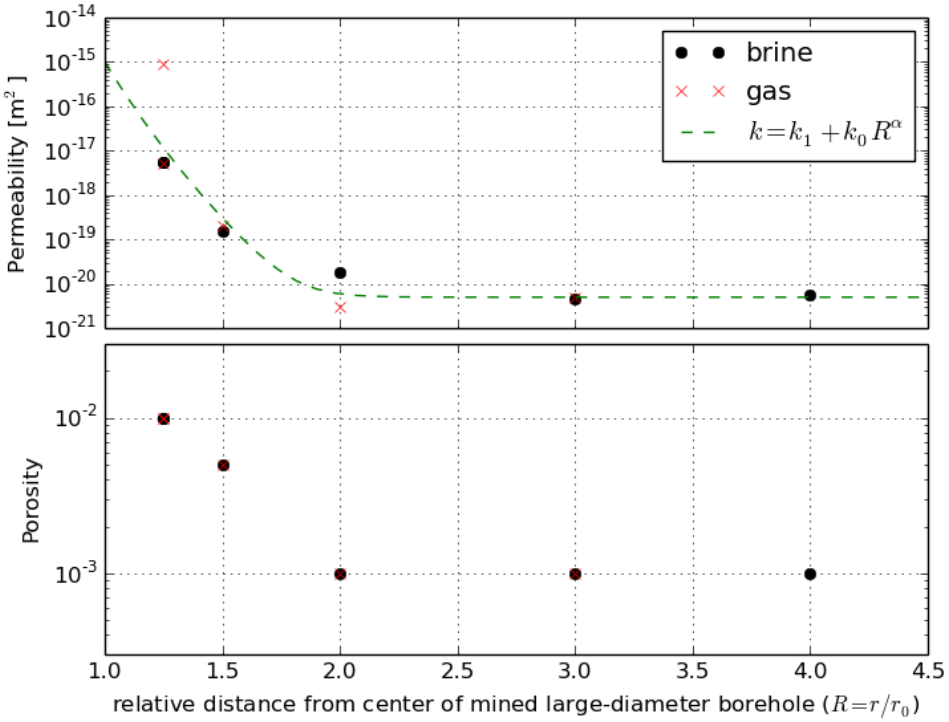


**Figure 2.11. Permeability and porosity estimates from small-scale mine-by test at WIPP (Stormont et al., 1991); power-law model suggested by Cosenza (1996)**

Porosity holds a special place among the parameters in the THMC problem, because it can be changed by several processes and it controls the extent of convection through the domain. Mechanical damage (i.e., volumetric strain) and healing can increase or decrease the porosity, along with chemical precipitation and dissolution. In many numerical models permeability is given simply as a power-law relation to porosity, despite significant data indicating otherwise (e.g., Figure 2.13, Kuhlman and Matteo, 2018). Heat conduction and mechanical deformation are the primary processes that do not explicitly depend on porosity, since they are effective through the solid matrix, as well as the open pore space. Heat convection, radiation, hydrologic processes, and chemical processes all depend explicitly on a connected gas- or liquid-filled porosity.

Porosity in undisturbed salt is associated with very small apertures (Figure 2.12), which tend to be dominated by surface forces (e.g., held or influenced by electrostatic forces associated with the mineral phase). Surface forces have been proposed as causing non-Darcy flow (Liu and Birkholzer, 2012), and may lead to the very small effective diffusion coefficients that would be associated with salt in the far field. The specific surface area (surface area per volume) is higher in tight pores. Granular salt backfilled in the excavation behaves much more like a traditional porous medium, and has lower specific surface area. Microfractures added to the salt due to damage tend to be planar structures, which also have a large amount of surface area, compared to volume.

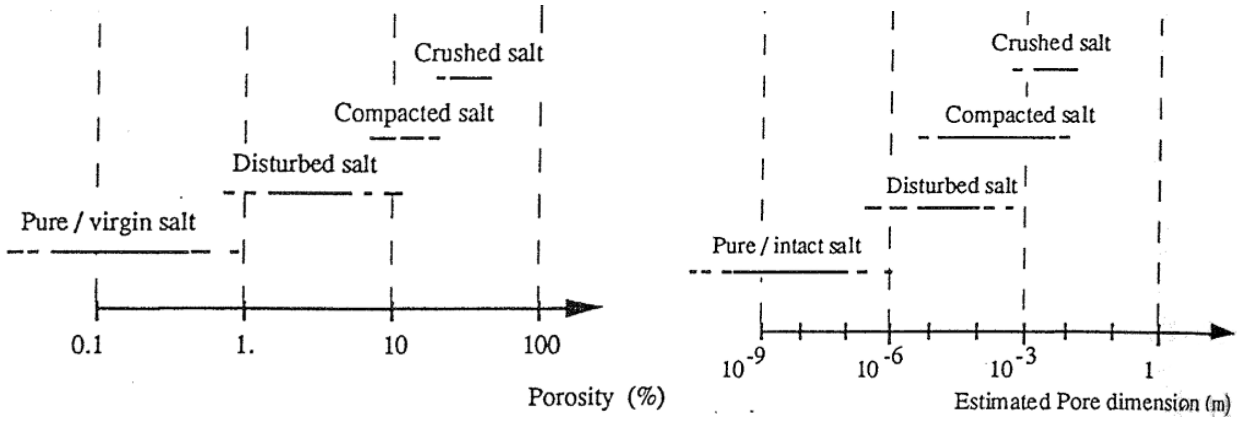


**Figure 2.12. Ranges of porosity and pore size in different regions around a salt excavation (Cosenza and Ghoreychi, 1993)**

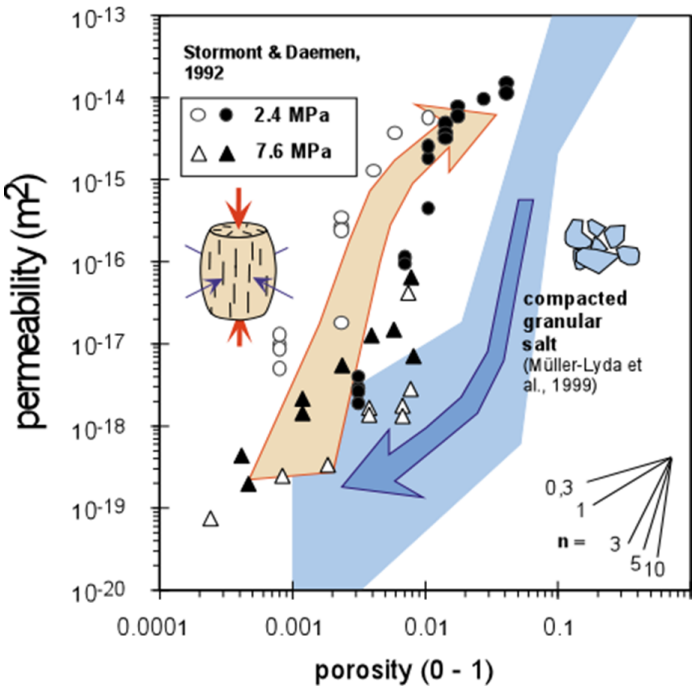


**Figure 2.13. Porosity-permeability data for dilating (orange) and reconsolidating (blue) salt (Popp et al., 2001)**

The connectivity of porosity in brine-saturated salt can also be impacted by the equilibrium dihedral angle (Lewis and Holness, 1996; Holness and Lewis, 1997). Under certain conditions (i.e., chemical equilibrium between the brine and solid phases), the connectivity of the porosity in salt is a function of pressure and temperature (Kuhlman et al., 2018). When the dihedral angle is above the critical value of 60°, geometric and thermodynamic arguments indicate porosity will not be connected (i.e., permeability will be nearly zero). The dihedral angle can go below the critical value (i.e., and permeability will increase) at pressures and temperatures found at depths below typical radioactive waste repositories (e.g., depths below 2 km at 100° C).

The pore-size distribution can be used to derive to the moisture retention curve, or relation-

ship between capillary pressure and saturation, and mostly impacts two-phase flow. It was stated above that porosity is an important variable that impacts anything occurring exclusively in the pore space, the pore-size distribution further describes this important backbone of hydrological processes, discriminating between granular and fracture-based media (Kuhlman and Matteo, 2018). As mechanical deformation (i.e., damage and healing) or chemical processese (i.e., precipitation and dissolution) occur in the salt, the porosity and permeability change, and the pore-size distribution should also change. Dissolution and precipitation will only occur in the smaller liquid-filled pores in a two-phase medium, preferentially changing these smaller pores. Mechanical deformation may occur differently in gas-filled pores compared to liquid-filled pores, based on impacts of fluid-assisted deformation and pressure solution. Further, the maximum capillary pressure of a formation that changes porosity significantly (i.e., during dissolution and precipitation) has been shown to be a function of porosity as well (Johnson et al., 2019).

## 2.3 Mechanical Processes

Mechanical deformation (i.e., strain) results from the configuration and changes in stress around an excavation, including damage accumulation, creep closure, and healing. The primary mechanical variables are stress and strain. In salt, strain is the creation of porosity while healing is the destruction of porosity. As discussed in the previous section, the modification of pore-size distribution, permeability, and tortuosity are typically not connected to geomechanical model output. These hydrological parameters are often simply related to porosity via power-law relationships.

The geomechanical problem is typically a balance of forces, usually ignoring inertial terms due to the very slow movements. The geomechanical problem then maps forces and stresses onto strains and displacements through one of many proposed constitutive laws (Reedlunn, 2016). Elastic stress-strain behavior in salt is instantaneous and it is a small component compared to long-term creep closure of excavations (Figure 2.14), although a large amount of nearly instantaneous elastic deformation happens when a room is first excavated due to the large stresses at depth.

We consider two different levels of mechanical model in salt:

- infinitesimal-deformation elastic and
- large-deformation with creep.

Only the large-deformation mechanical models that include creep closure are considered here as mechanical models for salt, since this type of behavior is important for salt. FEHM and PFLOTRAN both have some ability to simulation infinitesimal mechanical deformation, but are not considered mechanical models for salt without the ability to simulate creep and large deformation.

During viscoplastic creep the rock slowly deforms under a constant differential stress, like a very viscous fluid. The macroscopically observed transient and steady-state creep rate is due to several contributing small-scale processes (e.g., grain boundary sliding, dislocation creep, pressure solution creep, re-crystallization/healing), active at different pressures, temperatures, relative humidity, and strain rates (Munson and Dawson, 1981; Carter and Hansen, 1983). It is possible that each of these pore-scale mechanical deformation mechanisms contributes to volumetric strain (i.e., porosity), tortuosity, and pore-size distribution in a different way.

The mechanical initial condition before excavation is an undisturbed state, with the overburden stress the primary driving force. Since salt cannot support differential stress for long (i.e., creep will

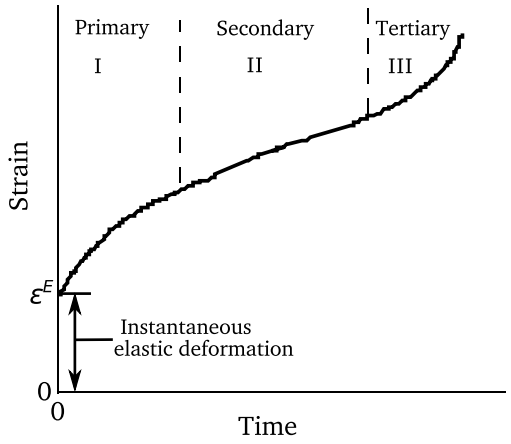


**Figure 2.14. Illustration of different stages of salt deformation. Stages I, II, and III are also called transient, steady-state, and damage creep**

tend to dissipate any differential stress), it will tend to be in a hydrostatic stress state in the far field. Mining out the underground excavation associated with the repository creates a large differential stress that creates the EDZ and drives creep closure. Figure 2.15 shows how the distribution of stresses ($\sigma$) around an excavation leads to the development of the EDZ (i.e., strain or porosity). The mechanical properties of the salt (i.e., Young's modulus, bulk modulus, shear modulus, Poisson ratio and creep constitutive law properties) may be considered to change smoothly as a function of strain or microfracturing across the DRZ to the far field. The Lux-Wolters constitutive model does this, but the Munson-Dawson constitutive model does not (Reedlunn, 2016, 2018).

The granular salt in a backfilled drift has different mechanical properties, but eventually the backfilled salt will also reconsolidate to the properties of intact salt in the far field.

Geomechanical models can be used to predict the distribution of damage (i.e., porosity) from creating an excavation, which is an important parameter for hydrological models or any process dependent on convection through the pore space. The distribution of damage around an excavation is a function of the depth of the excavation (i.e., lithostatic stress), the size and shape of the excavation (i.e., rounded vs. rectangular excavation – Figure 2.16), and any geologic heterogeneity associated with the salt (e.g., clay or anhydrite layers). Thin clay layers or any other interface between different materials can experience slip, which can impact the prediction of damage and closure at an excavation. Pore pressure in the clay layers reduces the effective normal stress clamping shut any slipping on the layer. Thermal pressurization could also increase slip on clay layers by increasing the pore pressure.

Mechanical models can consider elastic deformation (recoverable and non-damaging), viscoplastic creep (not resulting in damage if confined enough to be below the dilatancy criteria), and explicit damage or healing. In many mechanical constitutive models the mechanical strength properties do not diminish gradually with damage, but instead are lowered drastically when failure occurs. This type of constitutive law results in the mechanical EDZ being comparatively small and restricted to near the excavation, while the mechanically derived hydrological EDZ is larger (where strain and dilatancy occurs and influences the porosity).

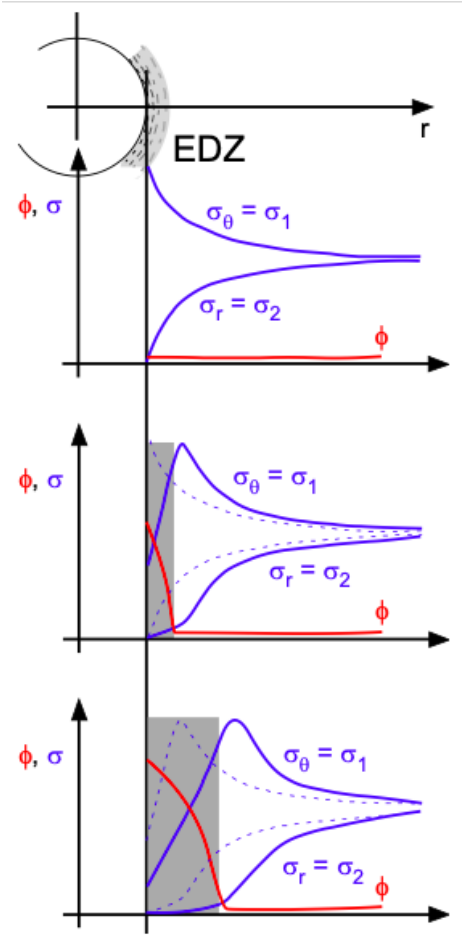


**Figure 2.15. Conceptual temporal evolution of stress ($\sigma$) and volumetric strain (porosity, $\phi$) contributing to mechanical EDZ (gray) around a salt excavation (Popp, 2019)**

## 2.4 Chemical Processes

The primary variables relevant to chemical liquid-phase transport are concentration or activity of different dissolved components (including dissolved radionuclides). The minerals making up the evaporite deposit (mostly halite, but significant anhydrite, polyhalite, clay may exist locally) and their heterogeneity are relevant to the chemistry.

As was mentioned for mechanical changes to porosity, relationships to pore-size distribution, permeability, and tortuosity are often not related to precipitation/dissolution predictions from chemical models, or only related through power-law relationships to porosity.

At WIPP, undisturbed fluid inclusions have a different compositional signature than intergranular brine, but the composition of fluid inclusions can change when they migrate under a thermal gradient (Caporuscio et al., 2013, 2014). Steam from boiling brine or dehydrating hydrous minerals can condense at cooler locations and re-dissolve salt. This re-dissolved brine is of very different composition (Kuhlman et al., 2018), since it is more closely related to the highly soluble solid minerals present (e.g., halite) than to the conate brines (i.e., concentrated ocean water from the Permian). Given these differences, it may be possible to discern the difference between the

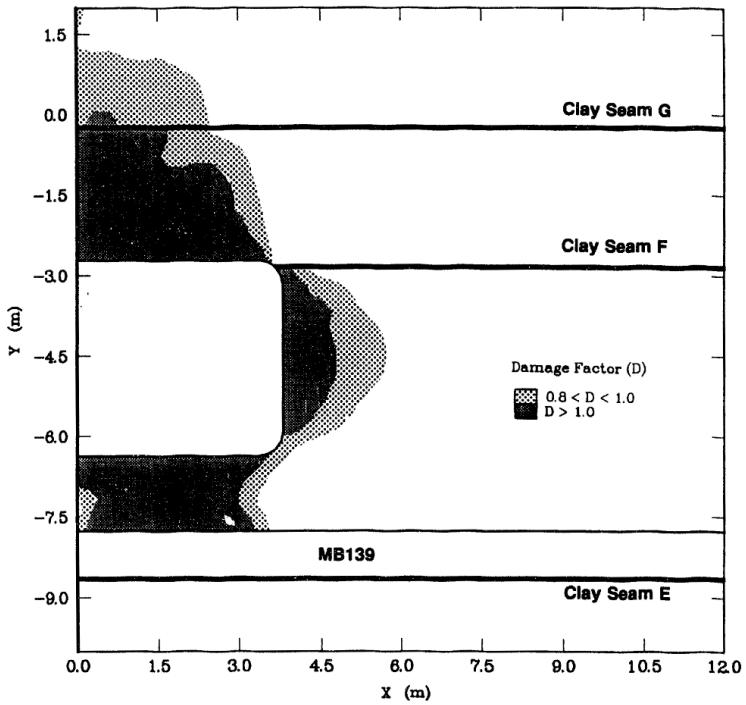


**Figure 2.16. Model prediction of damage around rectangular WIPP disposal rooms, including effects of non-salt layers (Van Sambeek et al., 1993)**

contributions of these water types given geochemical modeling (Kuhlman et al., 2018; Mills et al., 2019).

### 2.4.1 Reactive Transport

Reactive transport includes transport of dissolved species in the liquid phase, allowing species to react with each other and the solid phase during movement. The reaction-advection-diffusion equation is a set of $N$ reactions (one for each species), with each equation taking the form

$$\frac{\partial c_i}{\partial t} = D_{\text{eff}} \nabla^2 c_i + \vec{u} \nabla c_i + R_i$$

where $D_{\text{eff}} = D_m T^*$ is the effective diffusion coefficient and $R_i$ is a reaction term that accounts for radioactive decay, ingrowth, dissolution, precipitation, and reactions.

Gas-phase reactive transport is also possible (e.g., oxidation in the gas phase), but typically not considered in porous media subsurface simulations. Often the gas phase is treated in a simpler manner to the liquid phase, since most chemical reactions of interest happen in the liquid phase.

Reactive transport of solutes in the liquid phase is complicated by the very high ionic strengths in hyper-saline evaporite brines. To accurately predict mineral solubility and speciation at high ionic strengths and elevated temperatures require an activity model that accounts for more complex ion interactions, such as the Pitzer approach. The geochemical model EQ3/6 (Wolery and Jarek, 2003) has been used to predict the concentration of WIPP brines during the evaporation process at 50°, 75° and 100° C (Kuhlman et al., 2018). The thermodynamic databases require consistent data

across a range of temperatures and for the dissolved and mineral components of interest. Prediction of precipitation and dissolution of mineral also requires information on kinetic precipitation and dissolution rates for minerals of interest, possibly with different forward and backward rates as a function of temperature.

In most chemical modeling of salt systems (e.g., TOUGH-FLAC, FEHM, CODE_BRIGHT) where porosity is created and destroyed through precipitation and dissolution, variation in composition of the brine and salt are not explicitly tracked. The solid is considered to be pure halite, and the brine a saturated Na-Cl brine. The effects of temperature on solubility of minerals is not considered, nor are the different minor minerals found in WIPP salt or WIPP brine. As a first approximation, this is better than treating the salt as non-reactive, but the different minerals and components in the brine should be considered in a reactive transport simulation – especially one with significant heating and vapor transport.

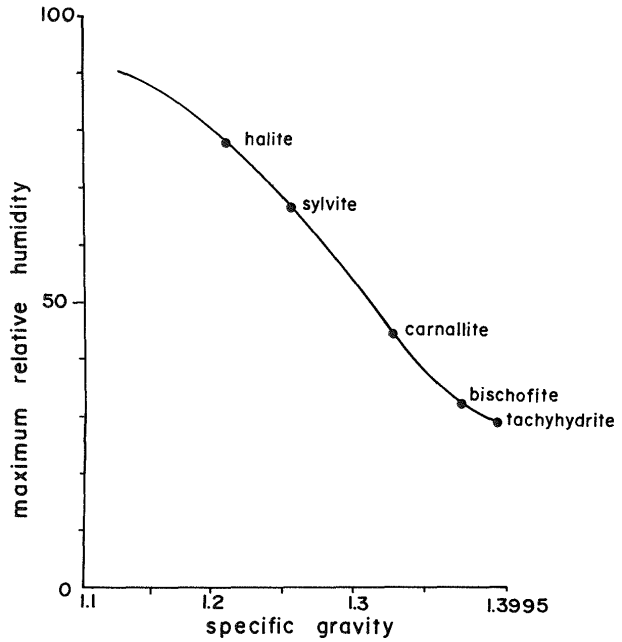


**Figure 2.17. Critical relative humidity and brine specific gravity during concentration of brine by evaporation (Sonnenfeld and Perthuisot, 1989)**

If a humid vapor is passed over a heterogeneous salt, depending on the relative humidity (RH), certain minerals will hygroscopically pull water from the air (i.e., water will condense from the air onto the mineral and if enough condensation occurs, it will cause the mineral to dissolve or *deliquesce*). Figure 2.17 shows the different equilibrium RH associated with common evaporite minerals associated with concentrating seawater. Halite has an equilibrium RH of $\approx 75\%$, which is approximately the steady-state humidity in a borehole or room with minimal ventilation in the WIPP underground (Jensen et al., 1993). Other more soluble minerals will deliquesce at this or even lower RH, such as sylvite ($KCl$), carnallite ($KMgCl_6 \cdot 6H_2O$), bischofite ($MgCl_2 \cdot 6H_2O$), and tachyhydrite ($CaMg_2Cl_6 \cdot 12H_2O$). While these minerals only exist in small amounts in WIPP salt, they will preferentially dissolve from moisture removed directly from humid air (i.e., in the air-saturated portion of the porosity), and can change the composition and physical properties (e.g., density and viscosity) of brines around a heat source. This figure also shows how brines at

different points along the evaporation curve have increasing specific gravity. As a brine is heated to evaporation near a heat source, it may tend to sink because of density contrast with surrounding brine. Furthermore, the temperature dependence of halite solubility in brine can lead to increases in permeability and porosity around a heat source, as the salt further dissolves into the heated brine (which would only occur in the brine-saturated porosity).

We distinguish here between geochemical modeling capabilities in THMC models, in increasing order of complexity:

- simulating advective, diffusive, and sorbing transport with possible radioactive decay of tracers or non-interacting solutes ($C_{REACT}$);
- simulating dissolution and precipitation, which modify the porosity and permeability ($C_{PPT/DIS}$);
- simulating "full chemistry" of the species found in the system (e.g., including pH), using thermodynamic and kinetic data to predict dissolution and precipitation of minerals ($C_{FULL}$).

THMC models that will include full chemistry information, needed for waste package corrosion or cementitous material degradation, are the most complex geochemical models. Fully coupled THMC process models may be used to screen processes for inclusion in PA simulations, and may ultimately be incorporated into PA simulations through multi-scale coupling (e.g., source term – near field coupling or near field – far field coupling), reduced order modeling, or surrogate modeling.

### 2.4.2 Chemical Transport Properties

Tortuosity is a measure of how long a flow path is through a porous medium, and mostly impacts diffusive transport (i.e., it relates the effective diffusion coefficient to the free-water or molecular diffusion coefficient). In the far field the effective diffusion coefficient is very low (i.e., nearly zero), as evidenced by compositionally different brines being juxtaposed by a few meters in evaporite deposits over geologic time (Roberts et al., 1999). In the near field the increased porosity and permeability are associated with tortuosity values that allows gas- or liquid-phase diffusion. Tortuosity is a metric of the nature of connectivity of a porous medium, which is a transport-centric description of the pore-space, beyond the information conveyed in the porosity, permeability, and pore-size distribution values.

Little is available on the tortuosity numerical values of the near- and far-field, and no information is available on how tortuosity changes with mechanical damage and healing of the excavations or chemical dissolution and precipitation in pore spaces. Flügge et al. (2016) presented results of laboratory diffusion experiments (cesium through brine) in recompacted granular salt (2% porosity). One result showed tortuosity values close to unity (i.e., effective diffusion coefficient equal to free-water diffusion coefficient), but other data they presented was harder to interpret (possibly showing the effects of precipitation and dissolution in the sample). In numerical models, often it is assumed tortuosity is a power-function of porosity and phase saturation (e.g., Millington and Quirk (1961)). More data on effective tortuosity of liquid and gas phases in granular, damaged, and intact salt would be useful for PA models.

Very low effective diffusion coefficients have been observed in other tight restrictive systems (e.g., zeolites), where a "configurational" diffusion (several orders of magnitude smaller than typi-

cal effective diffusion coefficients) is the only viable type of diffusion (Xiao and Wei, 1992; Webb, 2001).

# 3 Final Discussion

The mechanical deformation associated with excavating a repository imparts changes in porosity, permeability, and tortuosity that allow transport-related processes around the repository to exist. Chemical processes can further complicate things in a salt repository because dissolution and precipitation of evaporite minerals can further change porosity in the near field around a heater (e.g., a heat pipe).

| **Depending on porosity** | ***Not* depending on porosity** | **Changing porosity** |
|---|---|---|
| hydrological advection | heat conduction | mechanical (damage/healing) |
| heat convection | geomechanical deformation | chemical (dissolution/precipitation) |
| reactive transport | | hydrological (hydrofracture) |

**Table 3.1. Porosity dependence**

Table 3.1 lists processes that depend on porosity (left column) and those that modify porosity (right column). When chemical or thermal-chemical processes modify the porosity, how does this get updated in the mechanical model? In a loosely coupled THMC model, which process "owns" the porosity? These are some of the complexities in simulating coupled processes in a salt repository. An analogous (but more poorly defined) version of this table could be made for processes depending on and those impacting permeability, tortuosity, and the pore-size distribution (i.e., the moisture retention curve). Not all porosity (e.g., fracture porosity, granular porosity, matrix porosity) has the same equivalent transport behavior (Figure 2.13), and therefore porosity/permeability, porosity/tortuosity, and porosity/pore-size distribution relationships can be changed in different ways depending on whether a change to porosity was made by the mechanical model, the chemical model, or the hydrological model. Different micromechanisms of mechanical behavior may also have different impacts on different transport properties.

The hydrological problem has the largest change in material properties across the hydrologic EDZ and variables across the hydrologic EdZ. Other processes tend to have smaller associated damaged zones than the hydrologic problem. The mechanical process results in dilatancy or changes in porosity that impact the hydrological model, but this damage is typically not considered to have an impact on the mechanical properties themselves (except where failure is explicitly accounted for in mechanical constitutive models) – geomechanical models do not all include reduction of rock strength properties with small increases in damage.

The processes in a salt repository can be grossly divided into those that require porosity and those that do not. Mechanical deformation and heat conduction do not require a connected porosity (Table 3.1), and therefore could be effective into the far field. The processes that require a

connected porosity can either operate in air-filled porosity or brine-filled porosity, which can both exist in the backfilled drift, in the EDZ around the drift, but they will not be effective into the far field.

The hydrological flow problem drives thermal convection and chemical convective processes (and only occurs where there is a connected gas- or brine-filled porosity). In GDSA models presented before (Mariner et al., 2015; Sevougian et al., 2016), the far-field hydrological properties allowed more groundwater flow and solute diffusion than other evidence has shown is justified (Bollingerfehr et al., 2013). Future GDSA models should consider modifying these assumptions. Non-Darcy flow in the far field would eliminate any convection unless a threshold gradient is exceeded (i.e., a regional pressure gradient can exist, but regional hydrologic flow, heat convection, and solute transport does not). It is possible the threshold gradients may be different in salt and non-salt layers, so clay or anhydrite interbeds could theoretically experience very slow regional groundwater convection. The tortuosity and associated effective diffusion coefficient in the salt should be made lower, to reflect the observations that diffusion of water through the salt is not effective at evening out chemical differences, even over millions of years.

Parameters that characterize $\mathrm{TH^2MC_{FULL}}$ coupling should be investigated and better understood. Current coupling between mechanical and hydrological or chemical and hydrological models is done through porosity exclusively (i.e., tortuosity, permeability, and pore-size distributions are typically not modified by mechanical or chemical models directly). Mechanical and chemical models can change porosity, but keeping track of the total porosity and the porosity/permeability, porosity/tortuosity, and porosity/pore-size distribution is even more difficult. New approaches to coupling are required, and further laboratory and field data are required to validate any new approaches.

# Bibliography

Beauheim, R. L. and Roberts, R. M. Hydrology and hydraulic properties of a bedded evaporite formation. *Journal of Hydrology*, 259(1):66–88, 2002.

Beauheim, R. L., Ait-Chalal, A., Vouille, G., Tijani, S.-M., McTigue, D. F., Brun-Yaba, C., Hassanizadeh, S. M., van der Gissen, G. M., Holtman, H., and Mollema, P. N. INTRAVAL phase 2 WIPP 1 test case report: Modeling of brine flow through halite at the Waste Isolation Pilot Plant site. SAND97–0788, Sandia National Laboratories, Albuquerque, NM, May 1997.

Bollingerfehr, W., Buhmann, D., Filbert, W., Keller, S., Krone, J., Lommerzheim, A., Mönig, J., Mrugalla, S., Müller-Hoeppe, N., Weber, J. R., and Wolf, J. Status of the safety concept and safety demonstration for an HLW repository in salt. TEC-15-2013-AB, Federal Ministry for Economic Affairs and Energy (BMWi), Peine, Germany, 2013.

Bradshaw, R. L. and McClain, W. C. Project Salt Vault: A demonstration of the disposal of high-activity solidified wastes in underground salt mines. ORNL-4555, Oak Ridge National Laboratory, Oak Ridge, TN, 1971.

Bradshaw, R. L. and Sanchez, F. Migration of brine cavities in rock salt. *Journal of Geophysical Research*, 74(17):4209–4212, 1969.

Caporuscio, F. A., Boukhalfa, H., Cheshire, M. C., Jordan, A. B., and Ding, M. Brine migration experimental studies for salt repositories. LA-UR-13–27240, Los Alamos National Laboratory, Los Alamos, NM, September 2013.

Caporuscio, F. A., Boukhalfa, H., Cheshire, M. C., and Ding, M. Brine migration experimental studies for salt repositories. LA-UR-26603, Los Alamos National Laboratory, Los Alamos, NM, August 2014.

Carter, N. L. and Hansen, F. D. Creep of rocksalt. *Tectonphysics*, 92:275–333, 1983.

Cinar, Y., Pusch, G., and Reitenbach, V. Petrophysical and capillary properties of compacted salt. *Transport in Porous Media*, 64(2):199–228, 2006.

Cosenza, Ph. *Coupled Effects Between Mechanical Behavior and Mass Transfer Phenomena in Rock Salt*. PhD thesis, Ecole Polytechnique, 1996.

Cosenza, Ph. and Ghoreychi, M. Coupling between mechanical behavior and transfer phenomena in salt. In Ghoreychi, M., editor, *3rd Conference on Mechanical Behavior of Salt*, pages 271–293. Trans Tech Publications, 1993.

Davies, P. B. Evaluation of the role of threshold pressure in controlling flow of waste generated gas into bedded salt at the Waste Isolation Pilot Plant. SAND90–3246, Sandia National Laboratories, Albuquerque, NM, 1991.

DOE. Compliance recertification application 2014 for the Waste Isolation Pilot Plant. DOE/WIPP-14-3503, US Department of Energy, Office of Environmental Management, Carlsbad Field Office, Carlsbad, NM, 2014.

Flügge, J., Herr, S., Lauke, T., Meleshyn, A., Miehe, R., and Rübel, A. Diffusion in the pore water of compacted crushed salt. GRS-421, Gesellschaft für Anlagen- und Reaktorsicherheit (GRS) gGmbH, 2016.

Freeze, G., Gardner, W. P., Vaugh, P., Sevougian, S. D., Mariner, P., Mousseau, V., and Hammond, G. Enhancements to generic disposal system modeling capabilities. SAND2013-10532P, Sandia National Laboratories, Albuquerque, NM, 2013.

Freeze, G., Stein, E., Brady, P. V., Lopez, C., Sassani, D., Travis, K., and Gibb, F. Deep borehole disposal safety case. SAND2019-1915, Sandia National Laboratories, Albuquerque, NM, 2019.

Gloyna, E. F. and Reynolds, T. D. Permeability measurements of rock salt. *Journal of Geophysical Research*, 66(11):3913–3921, 1961.

Hadley, G. R. Theoretical treatment of evaporation front drying. *International Journal of Heat and Mass Transfer*, 25(10):1511–1522, 1982.

Hardin, E., Price, L., Kalinina, E., Hadgu, T., Ilgen, A., Bryan, C., Scaglione, J., Banerjee, K., Clarity, J., Jubin, R., Sobes, V., Howard, R., Carter, J., Severynse, T., and Perry, F. Summary of investigations on technical feasibility of direct disposal of dual-purpose canisters. FCRD-UFD-2015-000129 Rev. 0, Sandia National Laboratories, Albuquerque, NM, 2015.

Hardin, E. L., Clayton, D. J., Howard, R. L., Scaglione, J. M., Pierce, E., Manegee, K., Voegele, M. D., Greenberg, H. R., Wen, J., Buscheck, T. A., Carter, J. T., Severynse, T., and Nutt, W. M. Preliminary report on dual-purpose canister disposal alternatives (FY13). FCRD-UFD-2013-000171 Rev. 1, Sandia National Laboratories, Albuquerque, NM, 2013.

Herrera, I. and Pinder, G. F. *Mathematical modeling in science and engineering: An axiomatic approach*. John Wiley & Sons, 2012.

Hess, H. H., Adkins, J. N., Heroy, W. B., Benson, W. E., Hubbert, M. K., Frye, J. C., Russell, R. J., and Theis, C. V. The disposal of radioactive waste on land, report of the committee on waste disposal of the division of earth sciences. Publication 519, National Academy of Sciences - National Research Council, Washington, DC, 1957.

Holness, M. B. and Lewis, S. The structure of the halite-brine interface inferred from pressure and temperature variations of equilibrium dihedral angles in the halite-$H_2O$-$CO_2$ system. *Geochimica et Cosmochimica Acta*, 61(4):795–804, 1997.

Jenks, G. H. Effects of temperature, temperature gradients, stress, and irradiation on migration of brine inclusions in a salt repository. ORNL-5526, Oak Ridge National Laboratory, Oak Ridge, TN, 1979.

Jensen, A. L., Jones, R. L., Lorusso, E. N., and Howard, C. L. Large-scale brine inflow data report for Room Q prior to November 25, 1991. SAND92–1173, Sandia National Laboratories, Albuquerque, NM, 1993.

Johnson, K. S. and Gonzales, S. Salt deposits in the United States and regional geologic characteristics important for storage of radioactive waste. Y/OWI/SUB-7414/1, Office of Waste Isolation, Oak Ridge, TN, 1978.

Johnson, P. J., Zyvoloski, G. A., and Stauffer, P. H. Impact of a porosity-dependent retention function on simulations of porous flow. *Transport in Porous Media*, 127(1):211–232, 2019.

Kuhlman, K. L. Summary results for brine migration modeling performed by LANL, LBNL, and SNL for the used fuel disposition program. SAND2014-18217R, Sandia National Laboratories, Albuquerque, NM, 2014.

Kuhlman, K. L. and Malama, B. Brine flow in heated geologic salt. SAND2013–1944, Sandia National Laboratories, Albuquerque, NM, March 2013.

Kuhlman, K. L. and Matteo, E. N. Porosity and permeability: Literature review and summary. In *Mechanical Behavior of Salt IX*, Hannover, Germany, 2018. Federal Institute for Geosciences and Natural Resources.

Kuhlman, K. L. and Sevougian, S. D. Establishing the technical basis for disposal of heat-generating waste in salt. FCRD-UFD-2013–000233, US Department of Energy Used Fuel Disposition Campaign, Albuquerque, NM, 2013.

Kuhlman, K. L., Lopez, C. M., Mills, M. M., Rimsza, J. M., and Sassani, D. C. Evaluation of spent nuclear fuel disposition in salt (FY18). SAND2018-11355R, Sandia National Laboratories, Albuquerque, NM, 2018.

Lerch, C. Realistic modeling in R&D project KOMPASS – generic and/or specific. In *Tenth US/German Workshop on Salt Repository Researh, Design, and Operation*, 2019.

Lewis, S. and Holness, M. Equilibrium halite-$H_2O$ dihedral angles: High rock-salt permeability in the shallow crust? *Geology*, 24(5):431–434, 1996.

Liu, H. H. Non-Darcian flow in low-permeability media: key issues related to geological disposal of high-level nuclear waste in shale formations. *Hydrogeology Journal*, 22:1525–1534, 2014.

Liu, H.-H. and Birkholzer, J. On the relationship between water flux and hydraulic gradient for unsaturated and saturated clay. *Journal of hydrology*, 475:242–247, 2012.

Mariner, P. E., Gardner, W. P., Hammond, G. E., Sevougian, S. D., and Stein, E. R. Application of generic disposal system models. SAND2015-10037R, Sandia National Laboratories, Albuquerque, NM, 2015.

McTigue, D. F. Thermoelastic response of fluid-saturated rock. *Journal of Geophysical Research*, 91(B9):9533–9542, 1986.

McTigue, D. F. Flow into a heated borehole in porous, thermoelastic rock: Analysis. *Water Resources Research*, 26(8):1763–1774, 1990.

Millington, R. J. and Quirk, J. P. Permeability of porous solids. *Transactions of the Faraday Society*, 57:1200–1207, 1961.

Mills, M., Kuhlman, K., Matteo, E., Herrick, C., Nemer, M., Heath, J., Xiong, Y., Paul, M., Stauffer, P., Boukhalfa, H., Guiltinan, E., Rahn, T., Weaver, D., Dozier, B., Otto, S., Rutqvist, J., Wu, Y., Ajo-Franklin, J., and Hu, M. Salt heater test (FY19). SAND2019-4814R, Sandia National Laboratories, 2019.

Munson, D. E. and Dawson, P. R. Salt-constitutive modeling using mechanism maps. SAND81–2196C, Sandia National Laboratories, Albuquerque, NM, 1981.

Nuclear Energy Agency. Natural analogues for safety cases of repositories in rock salt: Salt club workshop proceedings. NEA/RWM/R(2013)10, Nuclear Energy Agency Organisation for Economic Co-operation and Development, 2014.

Nuclear Energy Agency. Microbial influence on the performance of subsurface, salt-based radioactive waste repositories. NEA No. 7378, Nuclear Energy Agency Organisation for Economic Co-operation and Development, 2018.

Olander, D. R., Machiels, A. J., Balooch, M., and Yagnik, S. K. Thermal gradient migration of brine inclusions in synthetic alkali halide single crystals. *Journal of Applied Physics*, 53(1): 669–681, 1982.

Olivella, S., Castagna, S., Alonso, E. E., and Lloret, A. Porosity variations in saline media induced by temperature gradients: Experimental evidences and modelling. *Transport in Porous Media*, 90:763–777, 2011.

Perry, F. V., Kelley, R. E., Dobson, P. F., and Houseworth, J. E. Regional geology: A GIS database for alternative host rocks and potential siting guidelines. FCRD-UFD-2014-000068, Los Alamos National Laboratory, Los Alamos, NM, 2014.

Popp, T. Natural closure of salt openings. In *Tenth US/German Workshop on Salt Repository Researh, Design, and Operation*, 2019.

Popp, T., Kern, H., and Schulze, O. Evolution of dilatancy and permeability in rock salt during hydrostatic compaction and triaxial deformation. *Journal of Geophysical Research*, 106(B3): 4061–4078, 2001.

Prevost, J. H. Two-way coupling in reservoir-geomechanical models: Vertex-centered Galerkin geomechanical model cell-centered and vertex-centered finite volume reservoir models. *International Journal for Numerical Methods in Engineering*, 98:612–624, 2014.

Ratigan, J. L. A finite element formulation for brine transport in rock salt. *International Journal for Numerical and Analytical Methods in Geomechanics*, 8:225–241, 1984.

Reedlunn, B. Reinvestigation into closure predictions of Room D at the Waste Isolation Pilot Plant. SAND2016-9961, Sandia National Laboratories, Albuquerque, NM, 2016.

Reedlunn, B. Enhancements to the Munson-Dawson model for rock salt. SAND2018-12601, Sandia National Laboratories, Albuquerque, NM, 2018.

Reynolds, T. D. and Gloyna, E. F. Reactor fuel waste disposal project: Permeability of rock salt and creep of underground salt cavities. TID-12383, Atomic Energy Commission Division of Technical Information, Oak Ridge, TN, 1960.

Roberts, R. M., Beauheim, R. L., and Domski, P. S. Hydraulic testing of Salado formation evaporites at the Waste Isolation Pilot Plant Site: Final report. SAND98–2537, Sandia National Laboratories, Albuquerque, NM, 1999.

Roedder, E. and Bassett, R. L. Problems in determination of the water content of rock-salt samples and its significance in nuclear-waste storage siting. *Geology*, 9:525–530, 1981.

Rübel, A., Buhmann, D., Meleshyn, A., Mönig, J., and Spiessl, S. Aspects on the gas generation and migration in repositories for high level waste in salt formations. GRS-303, Gesellschaft für Anlagen- und Raktosicherheit (GRS), 2013.

Rutqvist, J., Hu, M., Wu, Y., Blanco-Martìn, L., and Birkholzer, J. Salt coupled THMC processes research activities at LBNL: FY2018 progress. LBNL-2001170, Lawrence Berkeley National Laboratory, Berkeley, CA, 2018.

Salzer, K., Popp, T., and Böhnel, H. Mechanical and permeability properties of highly precompacted granular salt bricks. In Lux, K.-H., Minkley, W., Wallner, M., and Hardy, H. R. Jr., editors, *Proceedings of the Sixth Conference on the Mechanical Behavior of Salt*, pages 239–248, Hannover, 2007. Francis & Taylor (Balkema).

Sandia National Laboratories. Evaluation of options for permanent geologic disposal of spent nuclear fuel and high-level radioactive waste in support of a comprehensive national fuel cycle strategy (2 volumes). FCRD-UFD-2013–000371 Rev 1, US Department of Energy Used Fuel Disposition Campaign, Albuquerque, NM, April 2014.

Serata, S. and Gloyna, E. F. Reactor Fuel Waste Disposal Project: Development of design principle for disposal of reactor fuel into underground salt cavities. Sanitary Engineering Research Laboratory, Civil Engineering Department, University of Texas, Austin, TX, 1959.

Sevougian, S. D., Stein, E. R., Gross, M. B., Hammond, G. E., Frederick, J. M., and Mariner, P. E. Status of progress made toward safety analysis and technical site evaluations for DOE managed HLW and SNF. SAND2016-11232R, Sandia National Laboratories, Albuquerque, NM, 2016.

Shefelbine, H. C. Brine migration: A summary report. SAND82–0152, Sandia National Laboratories, Albuquerque, NM, 1982.

Sherer, N. M. Proceedings of salt repository project's workshop on brine migration, University of California-Berkeley, April 17–19, 1985. PNL/SRP-SA 14341, Pacific Northwest National Laboratory, Richland, WA, 1987.

Sonnenfeld, P. and Perthuisot, J. P. *Brines and Evaporites*. American Geophysical Union, 1989.

Stauffer, P. H., Guiltinan, E. J., Bourret, S. M., and Zyvoloski, G. A. Salt thermal testing in heated boreholes: Experiments and simulations. LA-UR-19-22729, Los Alamos National Laboratory, Los Alamos, NM, 2019.

Stormont, J. C., Howard, C. L., and Daemen, J. J. K. In situ measurements of rock salt permeability changes due to nearby excavation. SAND90–3134, Sandia National Laboratories, Albuquerque, NM, 1991.

Tsang, C.-F. Introduction to coupled processes. In Tsang, C.-F., editor, *Coupled Processes Associated with Nuclear Waste Repositories*, pages 1–5. Academic, 1987.

Tsang, C.-F. Introductory editorial to the special issue on the DECOVALEX-THMC project. *Environmental Geology*, 57:1217–1219, 2009.

Van Sambeek, L. L., Luo, D. D., Lin, M. S., Ostrowski, W., and Oyenuga, D. Seal design alternatives study. SAND92–7340, Sandia National Laboratories, Albuquerque, NM, 1993.

Webb, S. J. Modification of TOUGH2 to include the Dusty Gas model for gas diffusion. SAND2001-3214, Sandia National Laboratories, Albuquerque, NM, 2001.

Wolery, T. and Jarek, R. EQ3/6, version 8.0, software user's manual. , US Department of Energy, Office of Civilian Radioactive Waste Management, Las Vegas, NV, 2003.

Xiao, J. and Wei, J. Diffusion mechanisms of hydrocarbons in zeolites – I. theory. *Chemical Engineering Science*, 47(5):1123–1141, 1992.

Zoback, M. *Reservoir Geomechanics*. Cambridge, 2007.